

SITE CHARACTERISTICS IN STRONG MOTION ACCELEROGRAMES

by Hiroshi Tajimi

Summary

The purpose of the paper is to present materials of site characteristics derived from strong motion accelerogrames. The analyses were performed on records at the Kushiro district meteorological observatory in Hokkaido and records at a warehouse in Tokyo. The former site is located on relatively hard ground of coastal plateau facing the Pacific ocean and has the elevation of about 30 meters. The latter is located on deeply soft layer and the warehouse is founded on pile foundations. The results are discussed on the response spectrum curves.

Diluvial Terrace Site (Kushiro)

Since 1961, the strong motion accelerographs of the "SMAC" type installed in the Kushiro district meteorological observatory have recorded many earthquake motions of moderate intensities. Table 1 shows data of these earthquakes, all of which were analyzed in this study.

In the earlier observation, a set of SMAC was mounted on a concrete base rest on the ground within the building, as shown in Fig. 1. Thereafter, another set was added and placed on the other base with a distance of about 30 meters apart from the building. Therefore, two accelerographs operated until the first one was removed on Oct. 1967. Both sets are distinguished in this paper by marking of "A" and "B" for the first and the second, respectively. No.10 record is an exceptional example, which was obtained by the SMAC installed near the Otanoshige bridge located at the west end of the Kushiro alluvial plain (see Fig. 3). This record was used for comparison with No.9 record, which was simultaneously taken at the Kushiro station.

Fig.4 is the epicenter map. Fig.5(a) and 5(b) are the tracings of records. In particular, No.2 record was taken during the Hiroo-Oki earthquake, April 23, 1961, which indicated the maximum accelerations of 0.38 g in the NS direction and 0.23 g in the EW direction. Nevertheless, there was no damage in the Kushiro district. This fact emphasized the necessity of investigation of the relationship between accelerations and damage. The soil profil and shear velocities measured at the Kushiro station site are shown in Fig. 2.⁽¹⁾

(1) K. Tazime et al, Report on Study of Earthquake Disasters in Hokkaido, 1 (1966)

Maximum Acceleration

As found in Table 1, the maximum accelerations observed at the Kushiro station were always remarkably large in comparison with those expected normally from the magnitude of earthquake and the epicentral distance. The same feature was observed at the Hiroo Station, which is also located on the diluvial terrace with the distance 120 km south-west of Kushiro. Table 1 includes the maximum accelerations at the Hiroo station as a reference.

Response Spectra

The computed response spectra are plotted graphically for the critical damping ratio $h = 0.05$ and 0.1 in Fig. 6 to 15, on which one can point out the following remarks:

1. A dominant peak is found near the period of 0.25 to 0.28 sec in every spectra, as shown in Table 2. In addition, spectrum curves drop off rapidly with increase of the period.
2. The dominant period of microtremors measured on the SMAC base "A" was 0.25 to 0.27 sec in the NS direction and 0.26 sec in the EW direction.⁽²⁾
3. Another peak on microtremors is found near the period of 0.14 to 0.16 sec. Probably this peak was produced from excitation of the first layer. The corresponding peak in earthquake motions is found at the period of 0.13 to 0.15 sec in some of response spectra, which are marked by a small circle in Table 2.
4. The response spectra exhibit furthermore the third peak near the period 0.6 sec. It is probable that this peak was generated by deeper layers. The earthquake records involving this peak are marked by a small circle in Table 2.
5. The period of T_{CR} , at which the response acceleration is equal to the input acceleration is shown in Table 2.

Average and Standard Deviation of Response Spectra

The average and standard deviation of 12 spectra for records measured by the "A" SMAC were computed for the purpose of evaluation of site characteristics from the response spectra. To do this, the acceleration spectrum S_A was normalized by means of dividing the spectral value by a base value. In this paper, the base value was defined by the root-mean-square acceleration given by

(2) Y. Sakai et al, Report on Study of Earthquake Disasters in Hokkaido, 1 (1966)

$$\ddot{y}_{rms} = \left[\frac{1}{T} \int_0^T \dot{y}(t)^2 dt \right]^{1/2} \quad T = 3.0 \text{ sec} \dots\dots\dots(1)$$

In this equation, the acceleration-time function $\dot{y}(t)$ was chosen so as to include the maximum acceleration within the duration time of 3 seconds. This duration time can cover a train of 10 waves, when it continues with the dominant period of 0.3 sec. Using thus normalized spectra for $h = 0.05$, the average and standard deviation were computed and plotted in Fig. 16, where the bold line indicates the average and the fine lines indicates the standard deviation from the average. In this figure, the standard deviation near the dominant period attains to 15 - 25 %. This value is approximately equal to that expected theoretically under the assumption of the stationary random process. From this reason, one can conclude that the earthquake motion treated here had a common power spectrum in the vicinity of the dominant period.

Relation Between Root-Mean-Square Acceleration and Maximum Acceleration

It is supposed that the root-mean-square acceleration \ddot{y}_{rms} is approximately linear to the maximum acceleration \ddot{y}_{max} . When the root-mean-square acceleration was computed from Eq.(1), the ratios $\mu = \ddot{y}_{max}/\ddot{y}_{rms}$ are presented in Table 3. Evidently, all the ratios are near to a constant and have the average value $\mu = 2.74$ and the standard deviation $\sigma = 0.137$.

Response Spectra of Hiroo-Oki Earthquake

The response spectra for the Hiroo-Oki earthquake are presented in Fig. 7. Fig. 17 involves furthermore the response spectrum for the vertical acceleration. It is found that the dominant period is 0.33 sec in the vertical acceleration as same as in the horizontal acceleration. It is noteworthy that the dominant period of this earthquake was larger than that for the smaller earthquakes which are above mentioned.

Comparison of Records at the Kushiro Station and at the Otanoshige Station

During the earthquake Nov. 4, 1967, the simultaneous records were obtained at the Kushiro station as well as the Otanoshige station. The maximum acceleration at the former station was 2.5 times that at the latter station. The response spectra for the both stations are shown in Figs. 14 and 15. Besides, the ratio of (Kushiro)/(Otanoshige) are plotted in Fig. 18, in which the ratio is taken for the nominal direction of NS and EW, because the orientations of both accelerographs are not identified in a rigorous

sense. Since the hypocentral distance to the both stations are approximately equal, the differences in accelerations seem to be reduced to the ground contions. It is noted that the ratio is much larger in the short period, while it approaches to unity in the long period. Especially, it attains the maximum 15 at the period of 0.25 sec in the NS direction.

Table 1 List of Earthquakes

no. of record	Date	Epicenter	Depth (km)	Magnitude	Station	Epicentral distance (km)	Maximum Acceleration (g)
1	Nov. 15, 1961	145.6 E 42.7 N	60	6.9	Kushiro, A	103	0.10
2	Apr. 23, 1962	143.9 E 42.2 N	60	7.0	Kushiro, A	98	0.38
3	Jul. 18, 1962	145.2 E 42.6 N	60	5.9	Kushiro, A	80	0.08
4	May 31, 1964	147.7 E 43.2 N	60	6.7	Kushiro, A	270	0.09
5	Oct. 26 1965	145.7 E 44.1 N	160	6.2	Kushiro, A	160	0.14
6	ditto				Kushiro, B	160	0.12
	ditto				Hiroo	280	0.10
7	Sep. 19 1967	145.1 E 43.0 N	90	5.9	Kushiro, A	56	0.11
8	ditto				Kushiro, B	56	0.12
	ditto				Hiroo	165	0.06
9	Nov. 4 1967	144.5 E 43.6 N	20	6.8	Kushiro, B	45	0.21
10	ditto				Otanoshige	45	0.08

Table 2 Peak periods and T_{cr} from response spectra, $h=0.05$

No. of earthq.	Direction	Predominant period(sec)	0.14-0.16 (sec)	0.6 (sec)	T_{cr}
1	NS	0.27		o	0.81
	EW	0.25		o	1.08
2	NS	0.33	o		0.61
	EW	0.27	o		0.57
3	NS	0.27	o	o	0.43
	EW	0.27	o	o	0.7
4	NS	0.29			0.45
	EW	0.27	o		0.53
5	NS	0.29			0.54
	EW	0.27			0.63
6	NS	0.23			0.49
	EW	0.2			0.44
7	NS	0.25			2.17
	EW	0.25	o		0.41
8	NS	-		o	0.43
	EW	0.25		o	0.36
9	NS	0.23	o	o	0.37
	EW	0.25	o		0.39
10	NS	-			1.08
	EW	-			0.63

Table 3

No. of earthq.	Direction	\ddot{y}_{\max} (gal)	\ddot{y}_{rms} (gal)	$\mu = \frac{\ddot{y}_{\max}}{\ddot{y}_{\text{rms}}}$
1	NS	100.0	35.6	2.8
	EW	76.2	30.8	2.5
2	NS	381.0	160.4	2.4
	EW	233.3	67.0	3.5
3	NS	78.1	25.2	3.1
	EW	65.6	19.3	3.4
4	NS	90.0	33.3	2.7
	EW	45.6	15.6	2.9
5	NS	141.4	53.9	2.6
	EW	81.4	34.1	2.4
6	NS	117.2	42.4	2.8
	EW	120.7	44.5	2.7
7	NS	108.8	50.3	2.2
	EW	88.1	49.6	1.8
8	NS	78.9	27.6	2.9
	EW	116.8	39.5	3.0
9	NS	172.6	60.1	2.9
	EW	210.0	77.7	2.7
Average				2.74
Variance				13.7%
10	NS	37.2	13.9	2.7
	EW	84.8	22.0	3.9

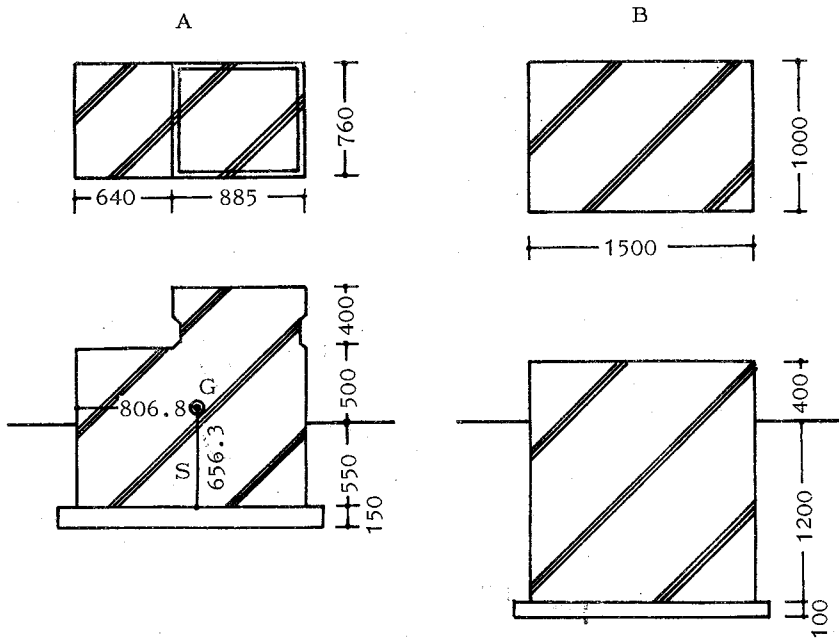


Fig. 1 Concrete bases for strong motion accelerographs (unit: mm)

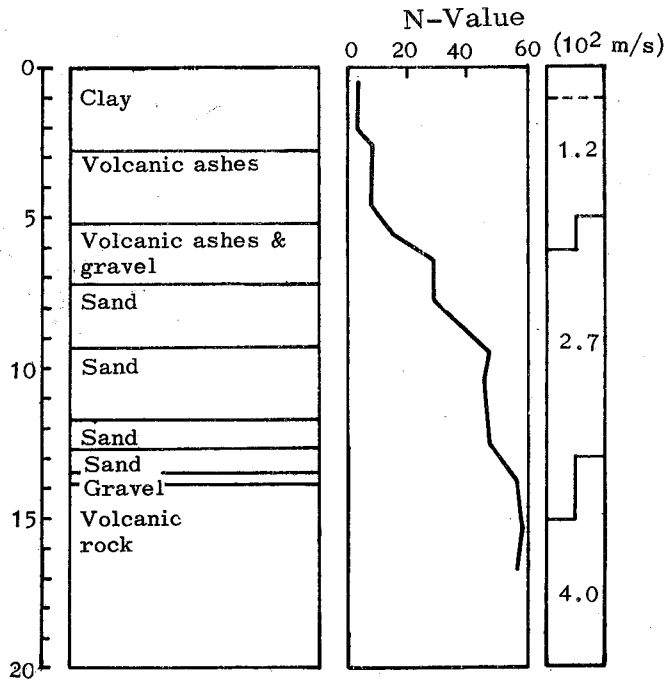


Fig. 2 Soil profiles of site and velocities of S-waves

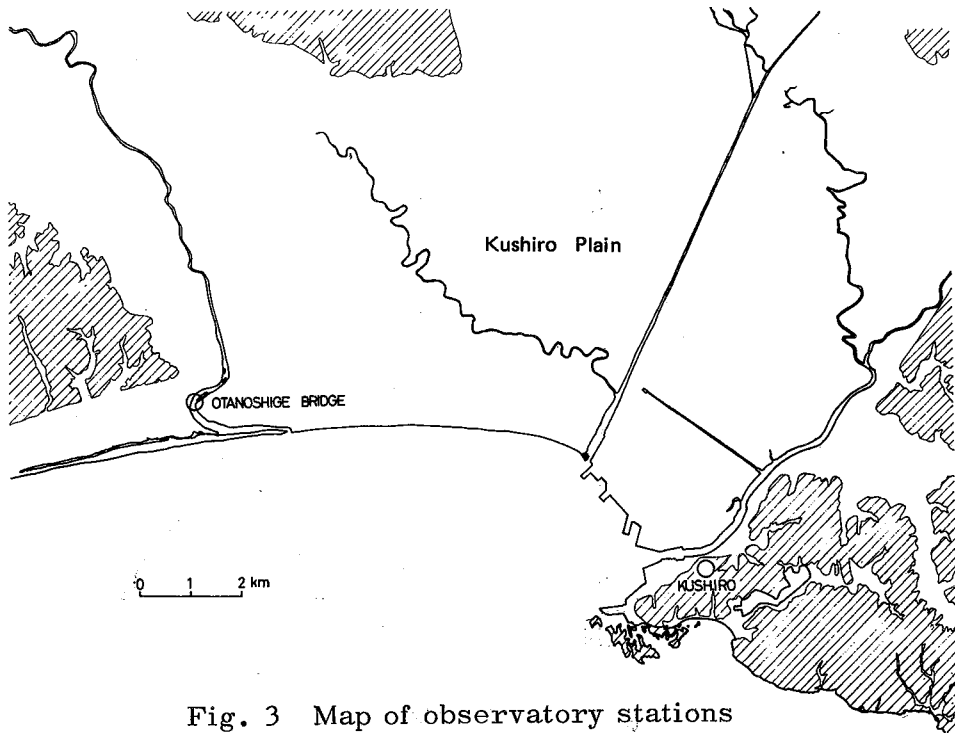


Fig. 3 Map of observatory stations

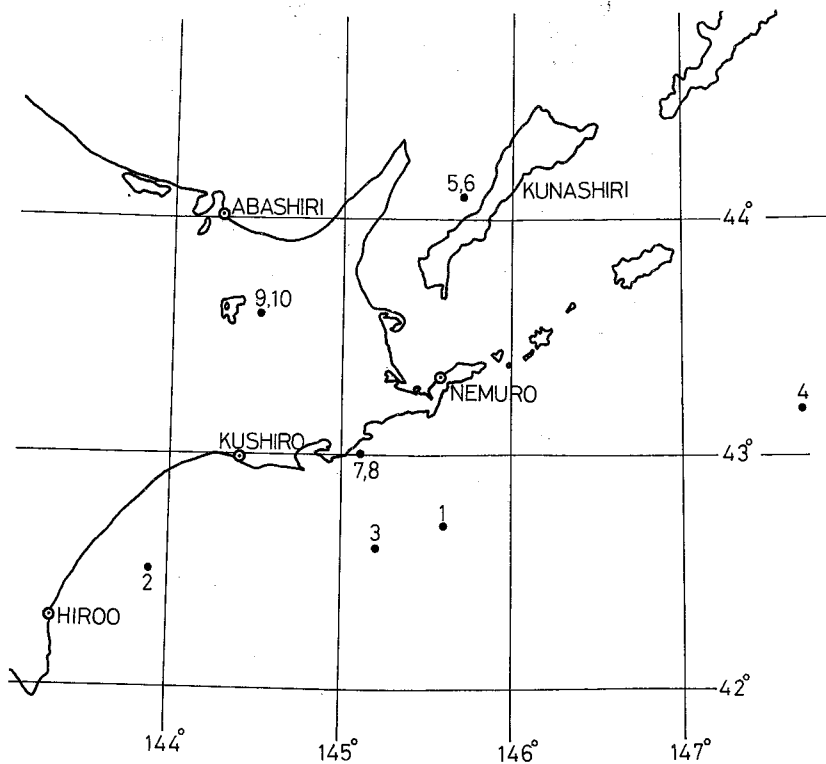


Fig. 4 Map of epicenters of earthquakes listed in Table 1

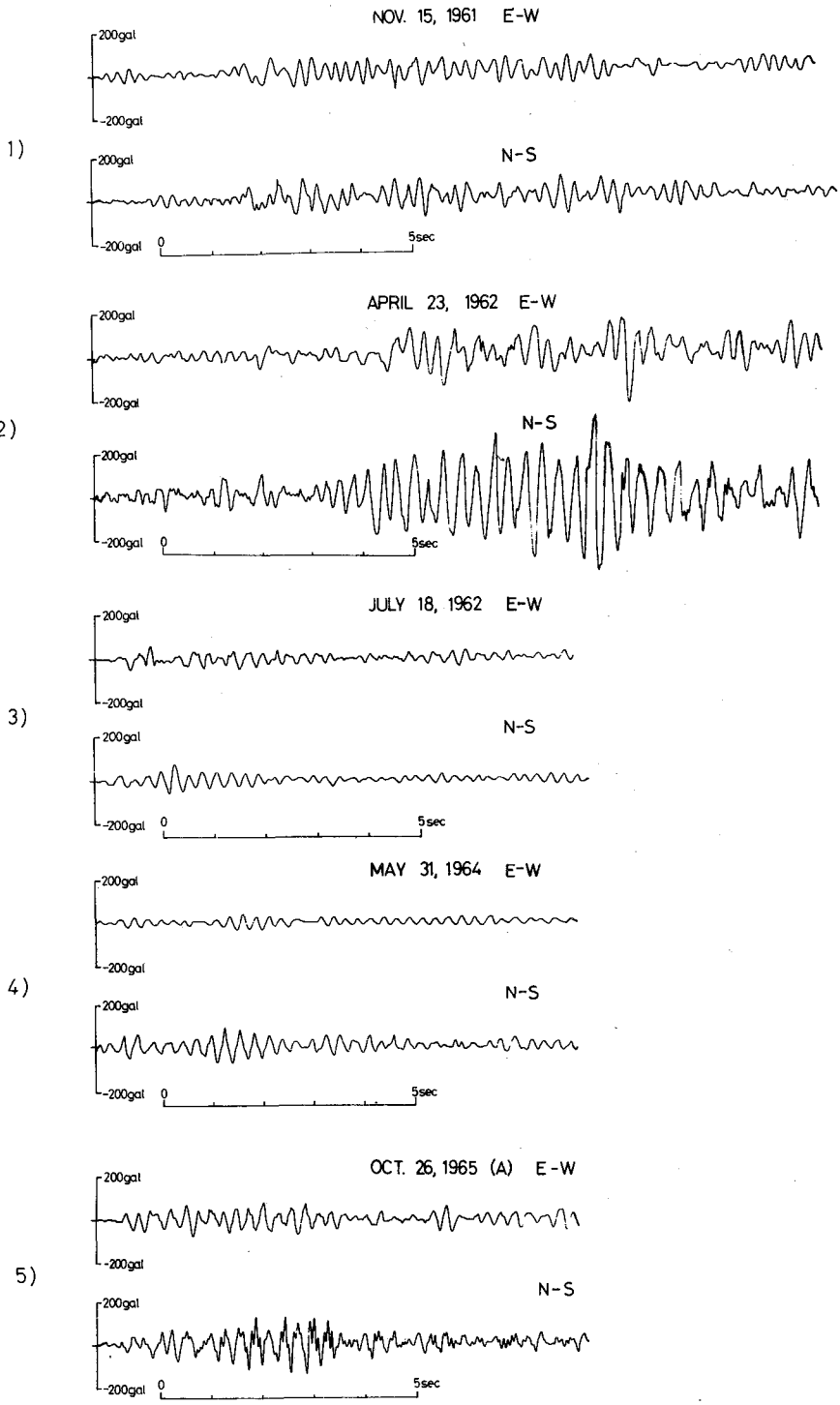


Fig. 5(a) Tracings of acceleration records

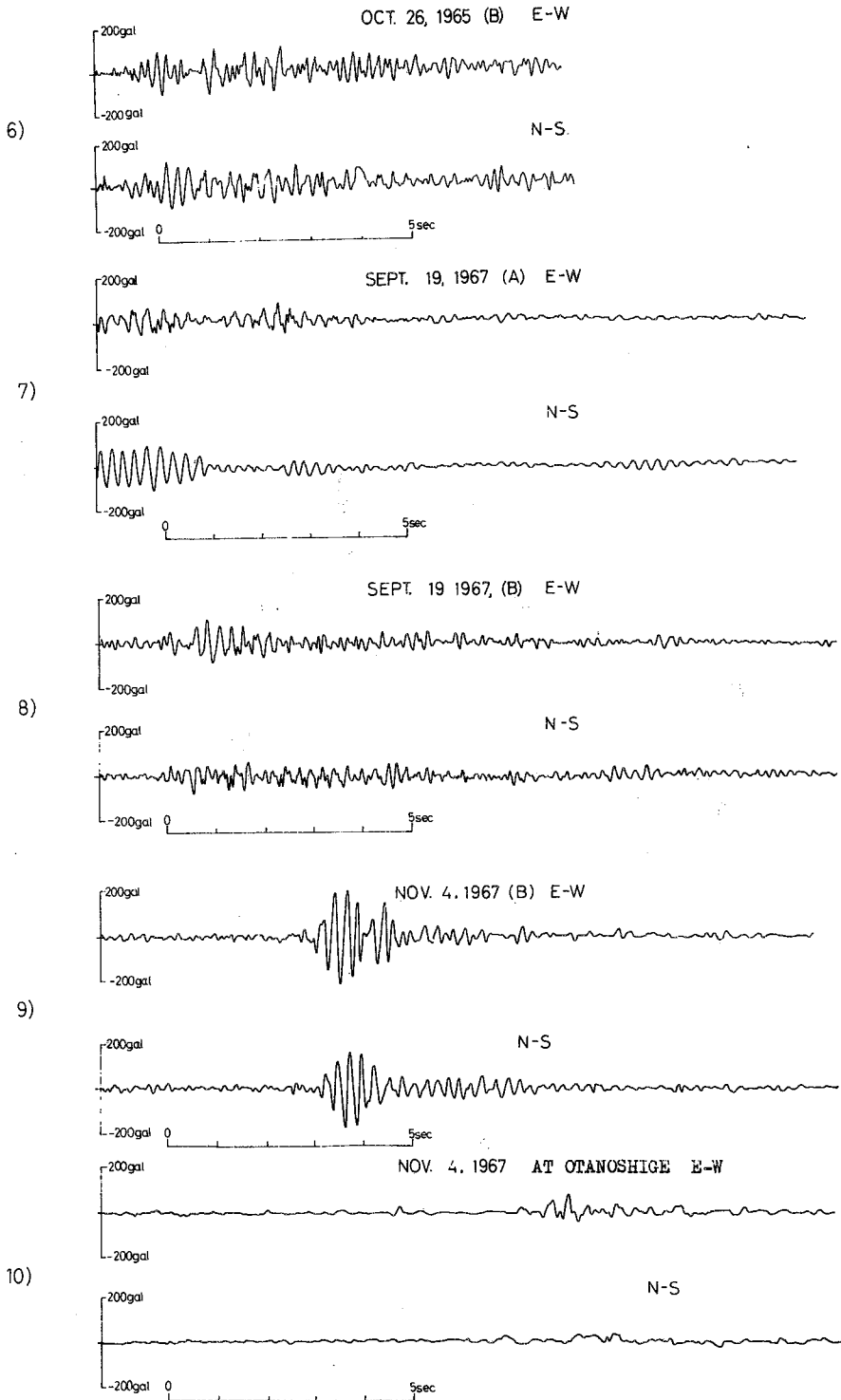


Fig. 5(b) Tracings of acceleration records

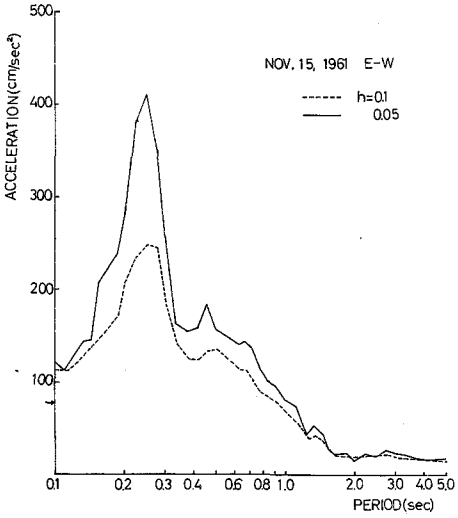
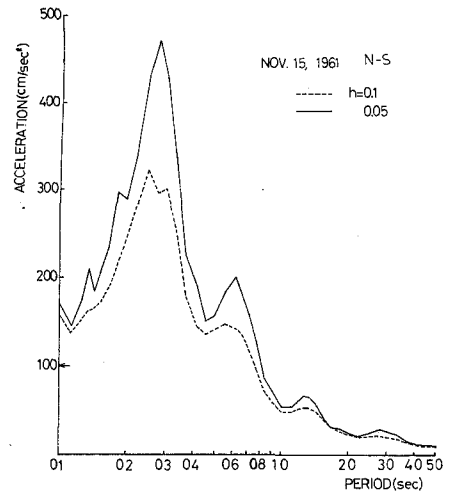


Fig. 6 Acceleration spectra of No.1 record

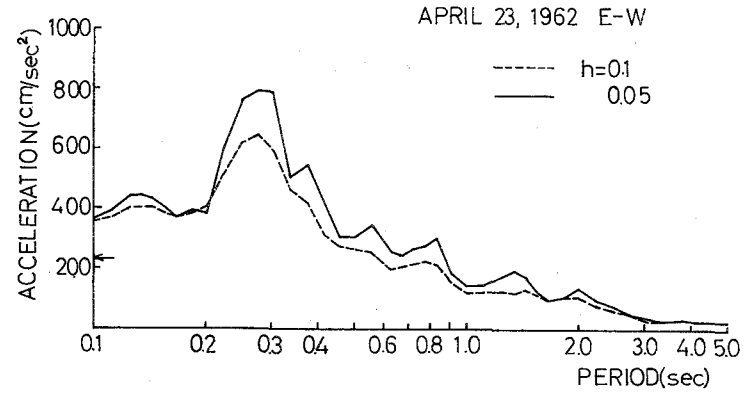
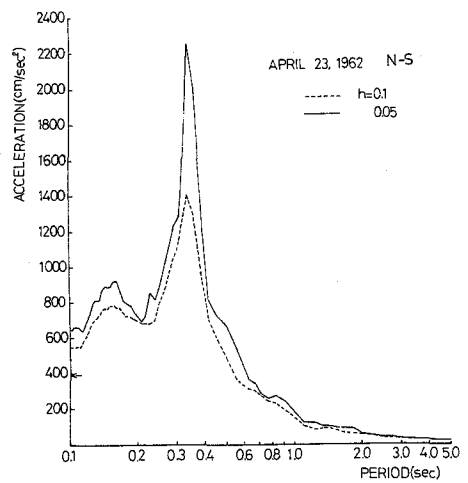


Fig. 7 Acceleration spectra of No.2 record

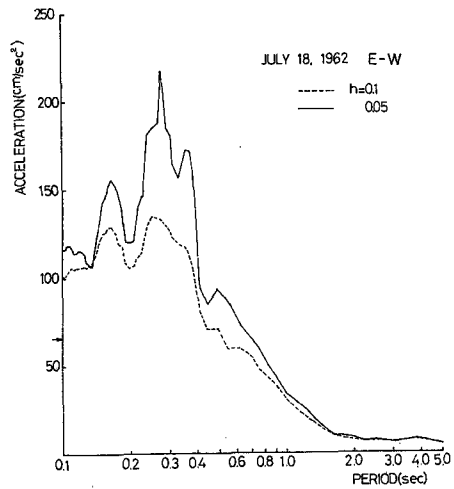
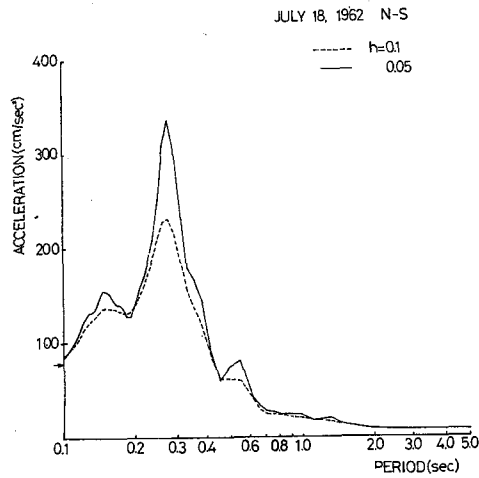


Fig. 8 Acceleration spectra of No.3 record

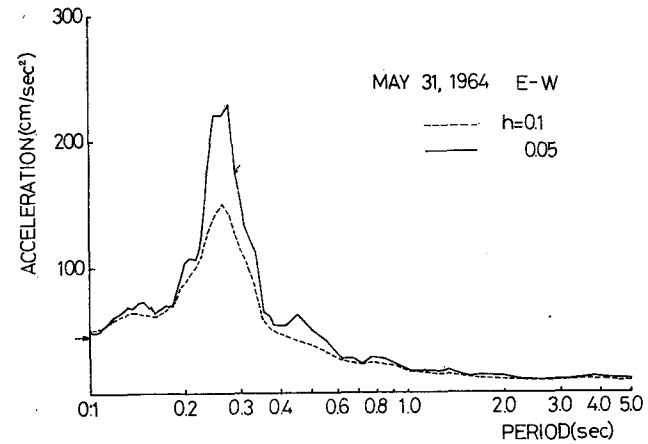
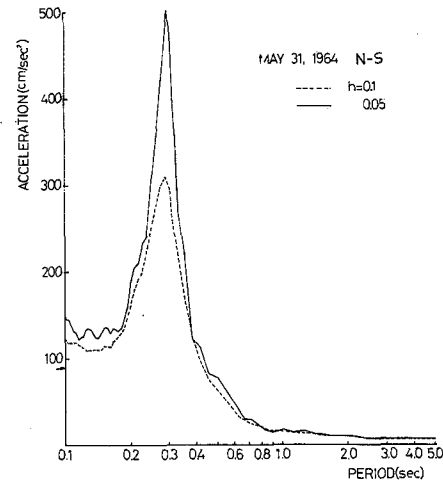


Fig. 9 Acceleration spectra of No.4 record

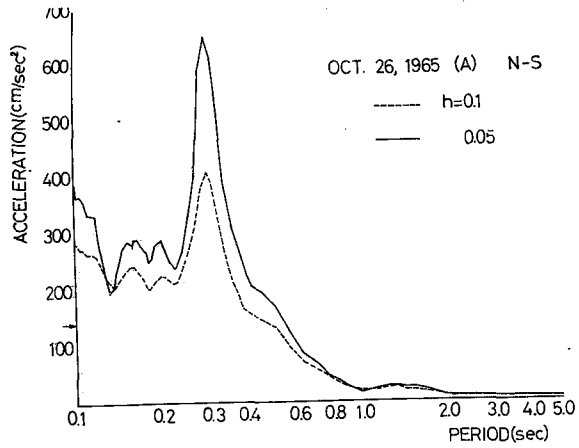


Fig. 10 Acceleration spectra of No.5 record

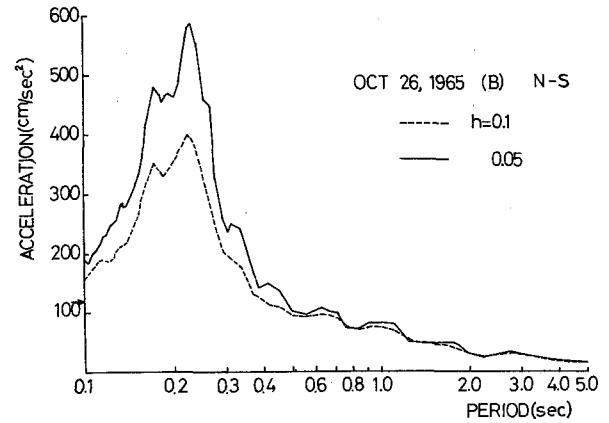
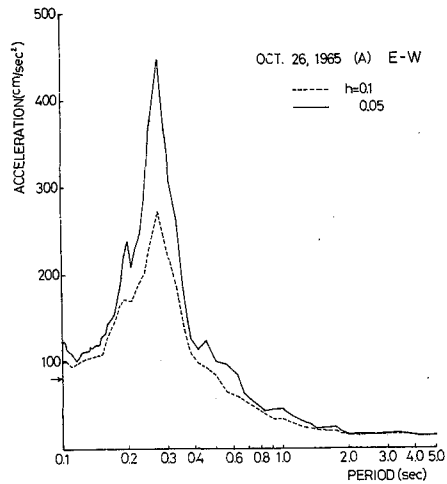
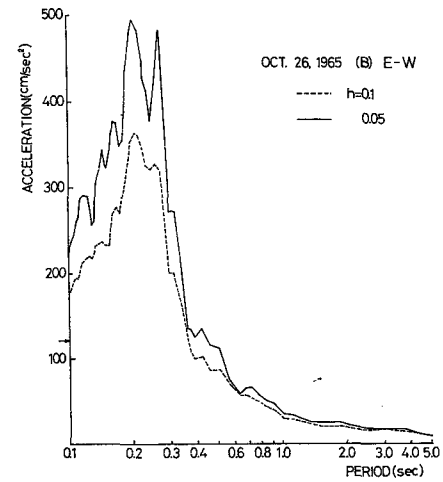


Fig. 11 Acceleration spectra of No.6 record



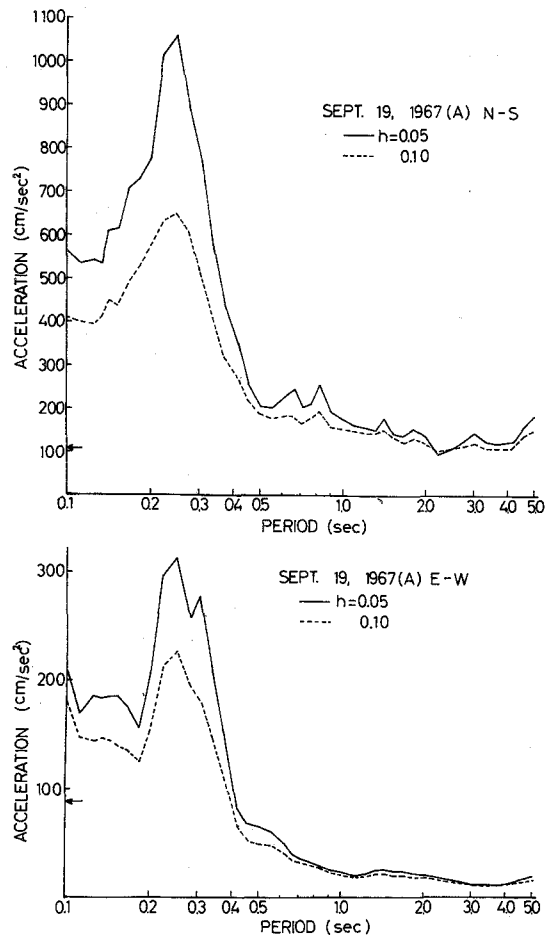


Fig. 12 Acceleration spectra of No. 7 record

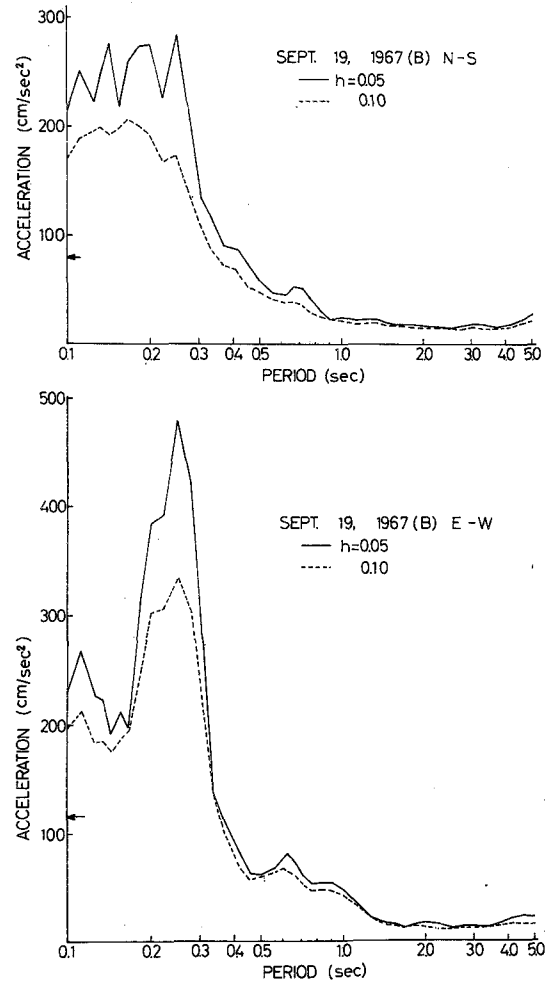


Fig. 13 Acceleration spectra of No. 8 record

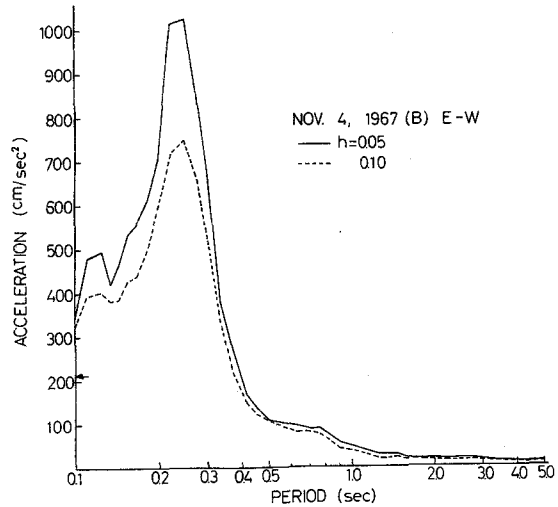
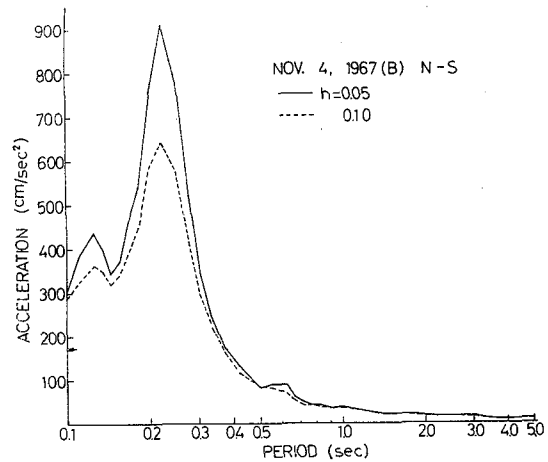


Fig. 14 Acceleration spectra of No. 9 record

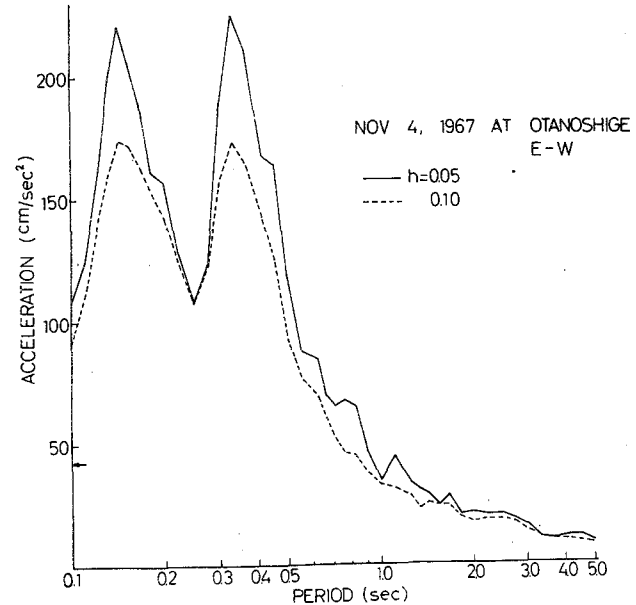
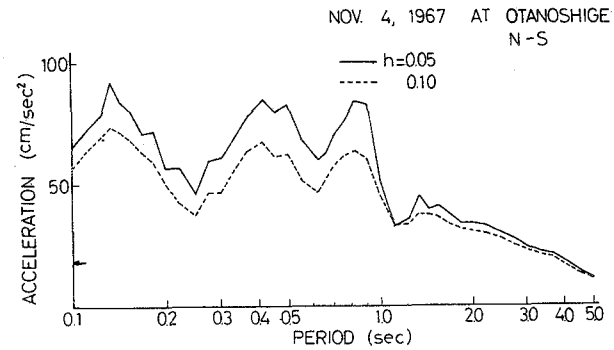


Fig. 15 Acceleration spectra of No. 10 record

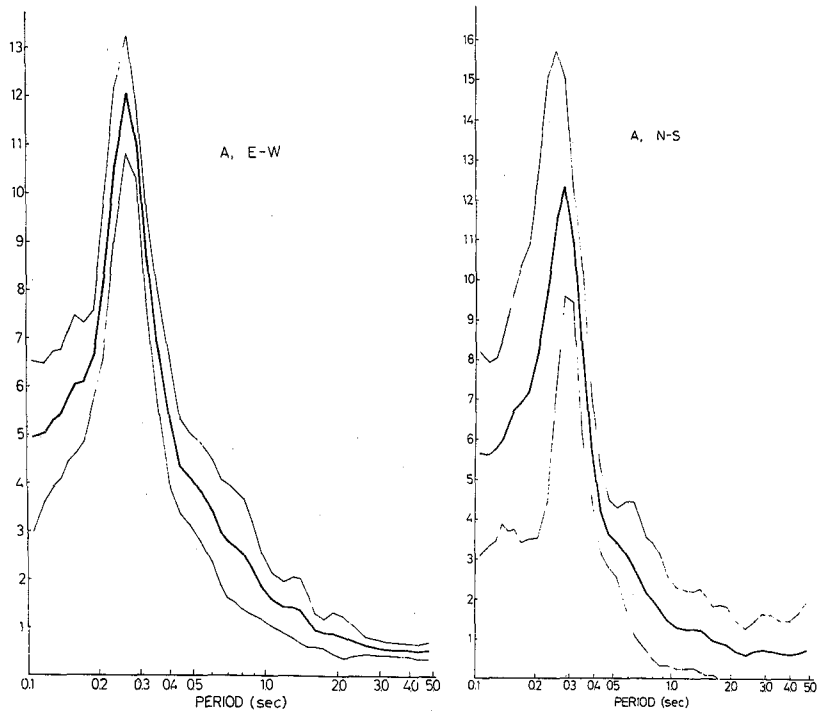


Fig. 16 Bold line show average curve for spectra.
Two fine lines show the distribution of
standard deviation from average spectra.

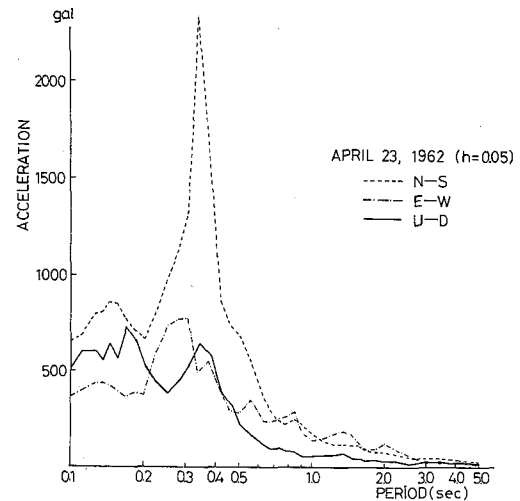


Fig. 17 Acceleration spectra

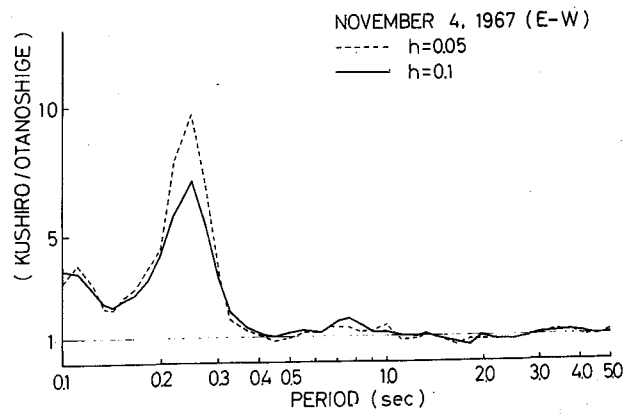
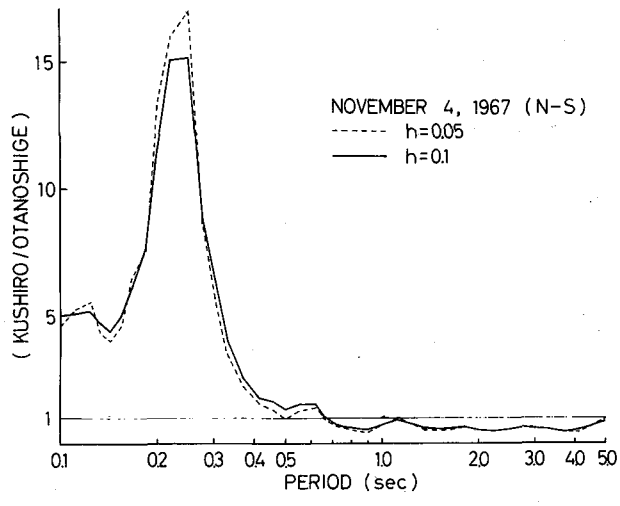


Fig. 18 Spectral ratio of records at the Kushiro station to those at the Otanoshige station

Deeply Soft Layer Site (Downtown of Tokyo)

The warehouse building is the four-storied rigid structure, 45.6 m by 60.8 m in area with column spacing of 7.6 m in the form of a square grid. The building belongs to Japan National Railway and is located at downtown in Tokyo. Three strong-motion seismographs (SMAC) are installed on the first floor, the third floor and the roof floor at an one position in the plan as shown in Fig. 19. The piles* passed through a soft peat and mud layer of 20 m thick and rest in a stiff fine sand layer of $N > 30$ (see Fig. 21).

Figs. 23 to 26 are plots of response spectra of acceleration for the first floor records and furthermore include diagrams of amplification ratio of spectrum for roof or third floor records to that for the first floor record. Fig. 27 collects response spectra of velocity for the first floor records. The damping ratio to the critical damping, which is used in the analysis, is $h = 0.05$.

It is evident that the velocity spectra for the EW direction in Fig. 27 have a pronounced peak at a period of 0.75 sec., although in case of the NS direction peaks are somewhat scattered. This period is surely the first mode period of the surface layer. Besides, there is a lower peak in the neighborhood of 0.35 sec. It is probably the period of translational mode of rigid structure-soil-piles system. The natural period of the superstructure is known from the peak period in a spectrum for the roof floor record. Table 1 shows the peak period for each earthquake and average values of them.

Table 4 Natural periods of superstructure (sec.)

Date	EW	NS
2 Mar. 1967	0.217	0.230
10 Nov. 1967	0.206	0.225
6 Mar. 1968	0.206	0.235
7 Mar. 1968	0.213	0.238
Average	0.21	0.23

* Concrete piles having a diameter of 50 cm and $I = 2.41 \times 10^5$ cm⁴

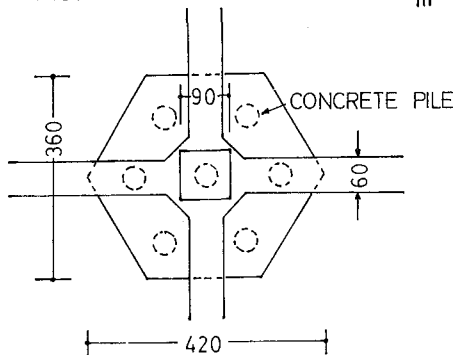
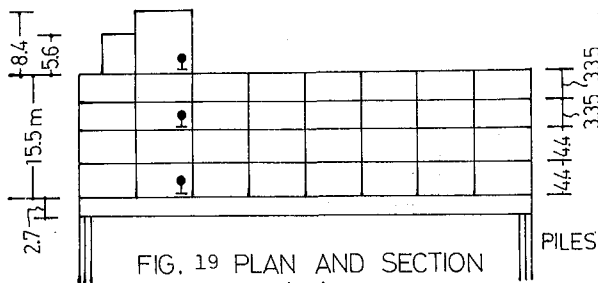
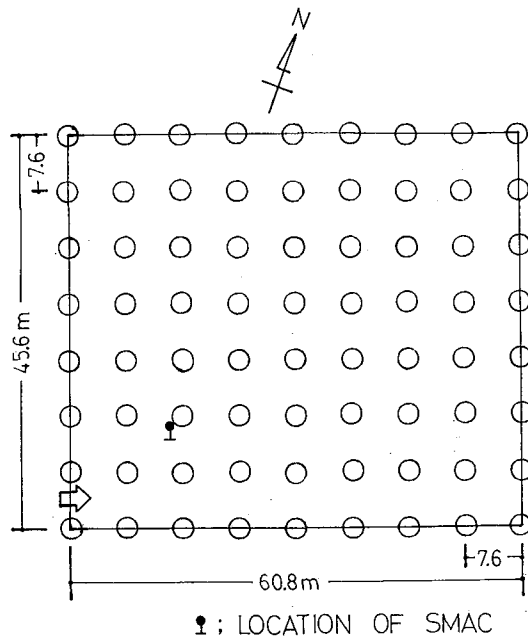


FIG. 20 TYPICAL FOOTING
 DIAMETER OF PILE ; 50cm
 TOTAL NUMBER OF PILES ; 437

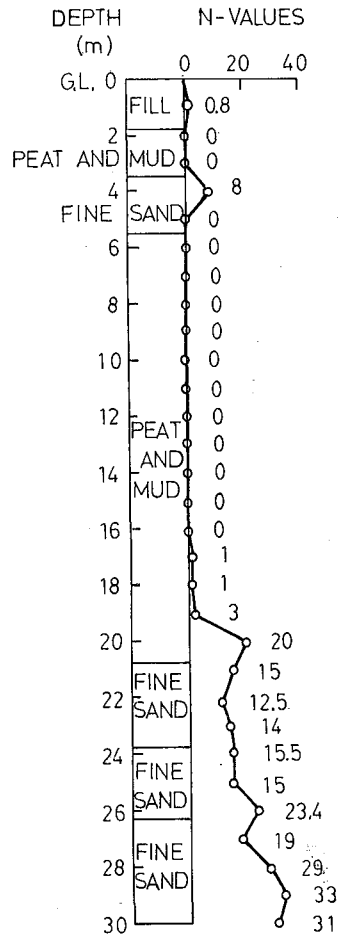


FIG. 21

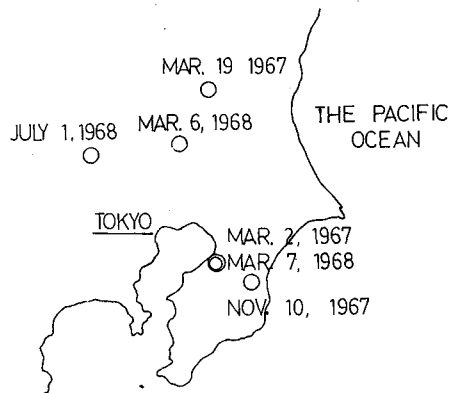


FIG. 22 EPICENTERS

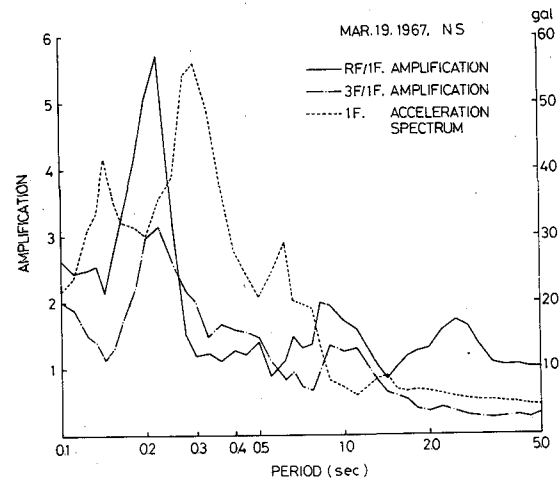
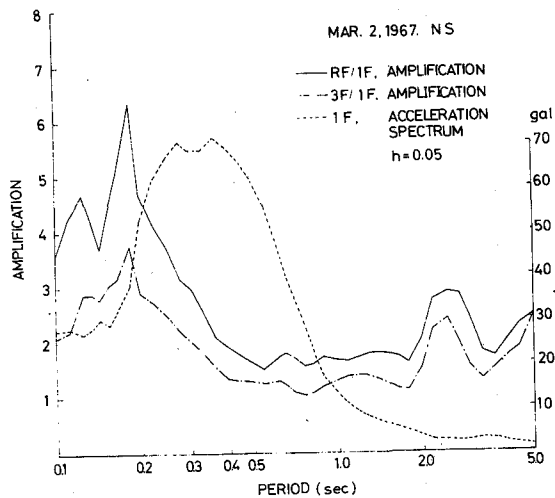
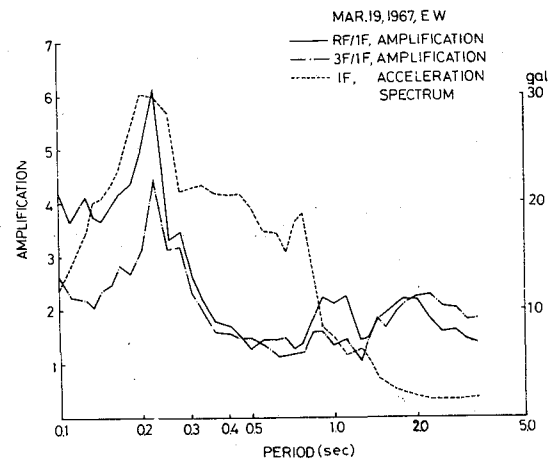
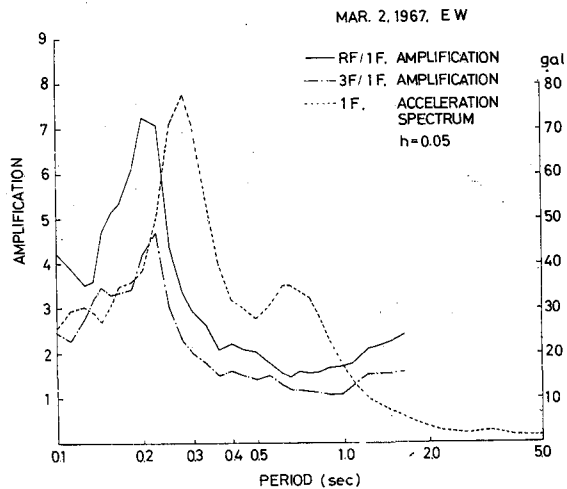
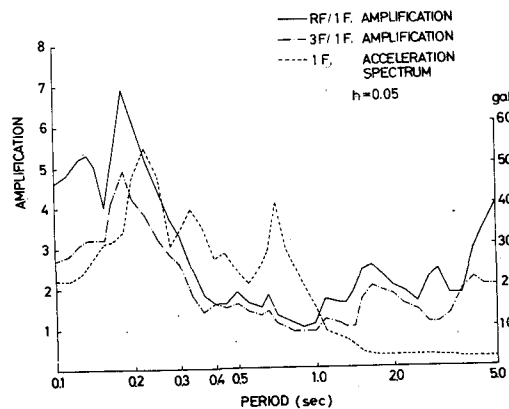


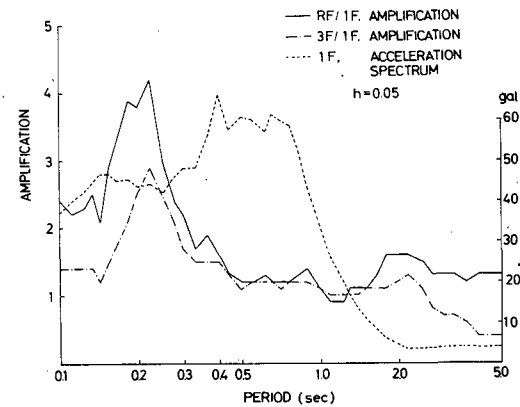
Fig. 23

Fig. 24

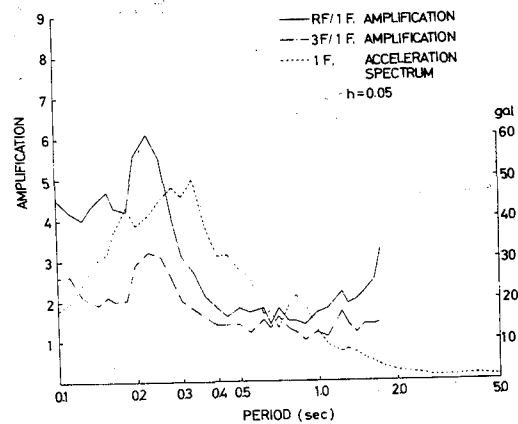
MAR. 6. 1968. EW



MAR. 7. 1968. EW



MAR. 6. 1968. NS



MAR. 7. 1968. NS

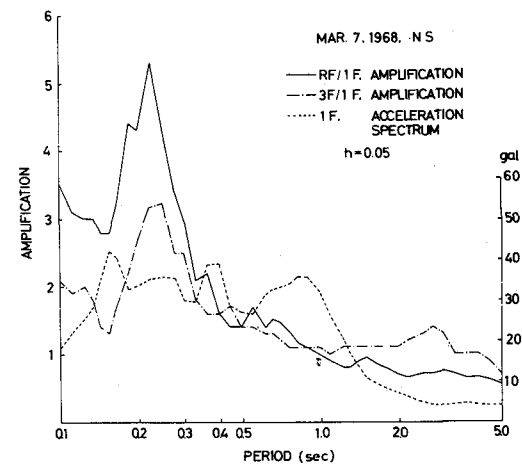


Fig. 25

Fig. 26

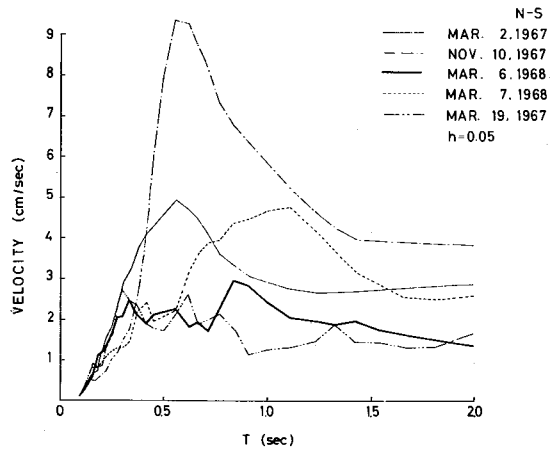
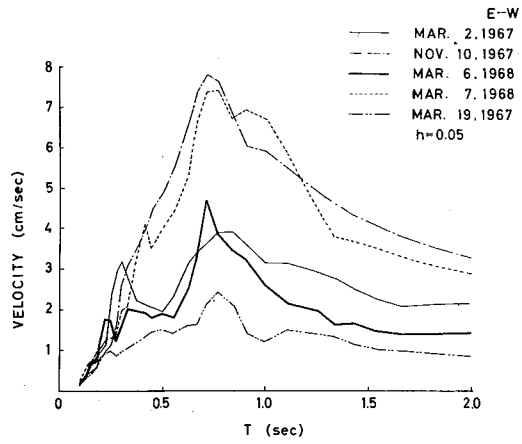


Fig. 27 Velocity spectra of the first floor records

Acknowledgements

I would like to express my deep appreciation to Prof. K. Kanai and members for inviting me to participate in the study of the Kushiro SMAC records. I am also indebted to Mr. H. Morita and Miss. A. Mizutani for help in processing the data.